A Method for Estimating Sea Surface Nitrate Concentrations from Remotely Sensed SST and Chlorophyll a—A Case Study for the North Pacific Ocean Using OCTS/ADEOS Data

Joaquim I. Goes, Toshiro Saino, Hiromi Oaku, and Ding Long Jiang

***Abstract*— We propose a method to estimate sea surface nitrate (N) from space using satellite measurements of sea surface temperature (SST) and chlorophyll a (chl a). The procedure relies on empirical relationships between shipboard measurements of N and its predictor variables, temperature (T) and chl a in surface and near surface waters. Although N appears to be controlled primarily by T, the addition of the biological variable chl a helps improve N prediction by reducing local and regional differences in the character of the temperature-nitrate (T-N) relationship. In the present study, we have applied these empirical algorithms to SST and chl a data from the Ocean Color and Temperature Scanner (OCTS) on board the Advanced Earth Observation Satellite (ADEOS). The results clearly suggest that measurements of SST and chl a now possible by modern-day ocean satellites could be exploited usefully to extend the resolution of shipboard N measurements over large spatial and temporal scales. Systematic errors in estimates of N that could result from errors in satellite estimates of SST and chl a are examined through sensitivity analyses.**

***Index Terms*— Algorithm, nitrogen, remote sensing, satellite, sea surface.**

I. Introduction

THE sinking of organic material produced by photosynthesis from the upper euphotic layers into the oceans interior represents a potential long-term sink for atmospheric CO_2 [1]. Its magnitude, is believed to be regulated by the supply of inorganic nitrogen, primarily nitrate (N) to the euphotic layer [1], [2]. For this reason, understanding the space and time variations of N availability in the euphotic layer is a valuable aspect of research concerning climate change. Despite its importance, N data sets obtainable by traditional shipboard techniques fall far short of the spatial and temporal scales required for global climate research. Satellites offer a promising tool toward this goal on account of their large and synoptic coverage. Unfortunately, no electromagnetic signal exists that can be exploited for directly measuring N from space [3]. However, the close relationship between N and certain variables that are now accessible to spaceborne sensors has led to the belief that satellites could be utilized to estimate N and extend the resolution of ship-based N estimates [4], [5].

One method that has been proposed takes advantage of the consistent negative correlation observed between T and N in localized data sets to estimate euphotic layer N concentrations from satellite sea surface temperature (SST) [6]–[9]. Empirical algorithms for N based on T-N relationships have been in existence for quite a while, but their application over large temporal and spatial domains has been restricted, due to the time and space varying nature of T-N relationships [3], [6]–[9]. A large database of shipboard measurements made by Japanese research vessels gave us an opportunity to reexamine T-N relationships in near surface and surface waters over a vast area of the Pacific Ocean. The results show that phytoplankton can account for a large measure of the variations in the character of the T-N relationship. We have used these findings to demonstrate that SST and chlorophyll a (chl a), now measurable by modern day satellites, when used in conjunction, could enable the production of high-quality maps of N in surface waters.

1) Background: The major input of N into the euphotic zone takes place when colder nutrient-rich deeper waters are brought up into the euphotic zone by upwelling and winter convective overturning, among other physical processes [10]. In the euphotic zone thereafter, incident solar radiation, a major source of heat for sea water warming and light for N uptake by phytoplankton, becomes a primary factor controlling its variability [10]. For this reason, correlations between T and concentrations of N have consistently been found to be negative and consequently, the focus of many attempts to estimate N concentrations from T. Estimations of

Manuscript received April 24, 1998; revised August 10, 1998. This work was supported by a Grant-in-aid for Scientific Research (Grant 96294) by the Ministry of Education, Science, Sports and Culture, Japan (Monbusho) and the National Space Development Agency (NASDA), Japan. The work of J. I. Goes was supported by a post-doctoral fellowship from the Japan Society for Promotion of Science, Japan.

J. I. Goes is with the Institute for Hydrospheric and Atmospheric Sciences, Nagoya University, Nagoya, Japan, and the National Institute of Oceanography, Dona Paula, Goa, India, 403004.

T. Saino is with the Institute for Hydrospheric and Atmospheric Sciences, Nagoya University, Nagoya, Japan, and the Earth Observation Research Centre, National Space Development Agency, Tokyo, Japan.

H. Oaku is with the Earth Observation Research Centre, National Space Development Agency, Tokyo, Japan.

D. L. Jiang is with the Institute for Hydrospheric and Atmospheric Sciences, Nagoya University, Nagoya, Japan.

Publisher Item Identifier S 0196-2892(99)03580-9.

TABLE I
SUMMARY OF SEA SURFACE (0 m) DATA SETS USED IN THE ANALYSIS. DEPTH-WISE DATA UP TO A MAXIMUM OF 50 m WAS USED ONLY IN CASES WHERE NO APPRECIABLE DIFFERENCES WERE OBSERVED IN BETWEEN SEA SURFACE TEMPERATURE AND SUBSURFACE TEMPERATURES

Date	Number of Stations	Ship Name	Region	Longitude Range	Latitude Range
May 1997	14	Tansei Maru	Sanriku ADEOS Field Campaign	142°E-145°E	39°N-41°N
July 1984 to August 1984	28	Tansei Maru	Izu-Island (Western North Pacific)	138°E-141°E	31°N-36°N
July 1985	26	Tansei Maru	Izu-Island (Western North Pacific)	138°E-141°E	32°N-34°N
June 1997 to Aug 1997	36	Kaiyo	Equatorial Pacific Ocean	140°E-180°E	10°N-10°S
Aug 1996 to Oct 1996	24	Hakurei Maru	Central Pacific Ocean	150°E-175°E	48°N-24°N
Aug 1993 to Oct 1993	42	Hakurei Maru	Central Pacific Ocean	175°E	48°N-15°S
Aug 1991 to Oct 1992	44	Hakurei Maru	Central Pacific Ocean	175°E	48°N-05°S
Aug 1992 to Oct 1992	35	Hakurei Maru	Central Pacific Ocean	175°E	48°N-15°S
June 1986 to Aug 1986	12	Hakuho Maru	Trans North Pacific Ocean	140°E-150°E	05°N-35°N
April 1986 to May 1986	7	Hakuho Maru	Western North Pacific Ocean	145°E-150°E	24°N-43°N
Aug 1983 to Sept 1983	17	Hakuho Maru	Western North Pacific Ocean	144°E-160°E	28°N-45°N
June 1978 to Aug 1978	11	Hakuho Maru	Trans North Pacific Ocean	140°E-150°E	52°N-35°N
Feb 1987 to Feb 1992	727	Kofu Maru	Western North Pacific	138°E-154°E	30°N-50°N
Sept 1990 to Oct 1990	51	Hakuho Maru	Eastern Equatorial Pacific Ocean	180°E-150°W	15°N-10°S
Nov 1994 to Jan 1995	26	Hakuho Maru	Southern Pacific Ocean	140°E-145°E	50°N-65°N

N based on T-N relationships have been found to be fairly precise when observations are restricted to small time and space domains [3], [6]–[9]. However, over large regional and basin scales, estimating N from T-N relationships has been limited because of the time and space varying nature of T-N relationships, believed to result largely from differences in the initial conditions of T and N in the source water [7] and/or due to variations in N uptake by phytoplankton [4]–[8]. In this study, using data collected during the Sanriku Field Campaign for validation of the Ocean Color and Temperature Scanner (OCTS) [11], we show that even when the area under investigation is confined to narrow space and time domains, the use of T-N relationships to characterize N may not necessarily hold true. We then use this information to present our case for addition of a term that would provide a measure for variations in N resulting from phytoplankton uptake and show that its inclusion in the predictive algorithm could help improve the accuracy of N estimations from space.

II. MATERIALS AND METHODS

1) Sanriku Field Campaign: The Sanriku field campaign for validation of the OCTS on board the Advanced Earth Observation Satellite (ADEOS) was undertaken in the western Pacific Ocean, off the coast of Sanriku, Japan, from May 7–14, 1997, on the research vessel *R/V Tansei Maru* (Table I). The survey yielded a comprehensive data set [11] of T, N, and chl a at 23 stations that spanned a range of water types, from the cold Oyashio waters in the north, to the warm Kuroshio waters in the south, and a region of mixed waters comprising the confluence of the northward flowing extension of the Kuroshio currents, the Kuroshio-Oyashio front, the warm core ring, and the mixed waters around and in the perimeter of the warm core ring [12].

2) Pacific Ocean Data Sets: The data sets for the Pacific Ocean utilized in this study were collected by Japanese oceanographic research vessels at different times of the year, during several cruises. The period of study and the approximate area covered during each cruise are presented in Table I. After quality checks, data sets from different cruises were pooled together, irrespective of the seasons and regions they were drawn from.

Since the focus of this study was on estimating sea surface N concentrations, our analysis was restricted to variables in surface sea water. However, data from the subsurface was included whenever differences between SST's and subsurface T values were minimal (<0.2 °C). Chl a was chosen as our predictor biological variable, largely because of its known relationship with N in the euphotic zone and its accessibility from space along with SST. Our choice of limiting this analysis to surface and near-surface waters is different from previous attempts to characterize N in seawater using data from deeper waters [5]–[9]. Yet, empirical algorithms for N based on surface and near-surface water properties appear to be a better choice for use with remotely sensed data as satellites perceive SST and chl a [13] best in the surface and in the upper layers, respectively. Our inclusion of chl a as a predictor variable also contrasts with previous attempts to model N solely on the basis of hydrographic properties such as SST, salinity, or density.

For the Sanriku Campaign data set, the final analysis was based on 39 data points, and for the Pacific Ocean data (including the Sanriku data set), 1822 data points. In both cases, the relationship between N and its predictor variables was examined using a step-wise linear regression fitting routine using the statistical package JMP.[1]

III. RESULTS AND DISCUSSION

A. Algorithm Development

1) Sanriku Field Campaign: With the Sanriku Field Campaign data set, we attempted to model N; first on the basis of the shipboard estimates of SST followed by SST in conjunction with chl a. From the results presented in Fig. 1(a), it is evident that even when the area under investigation is small, predictions of N based solely on T may not always

[1] JMP is a registered trademark of SAS Institute.

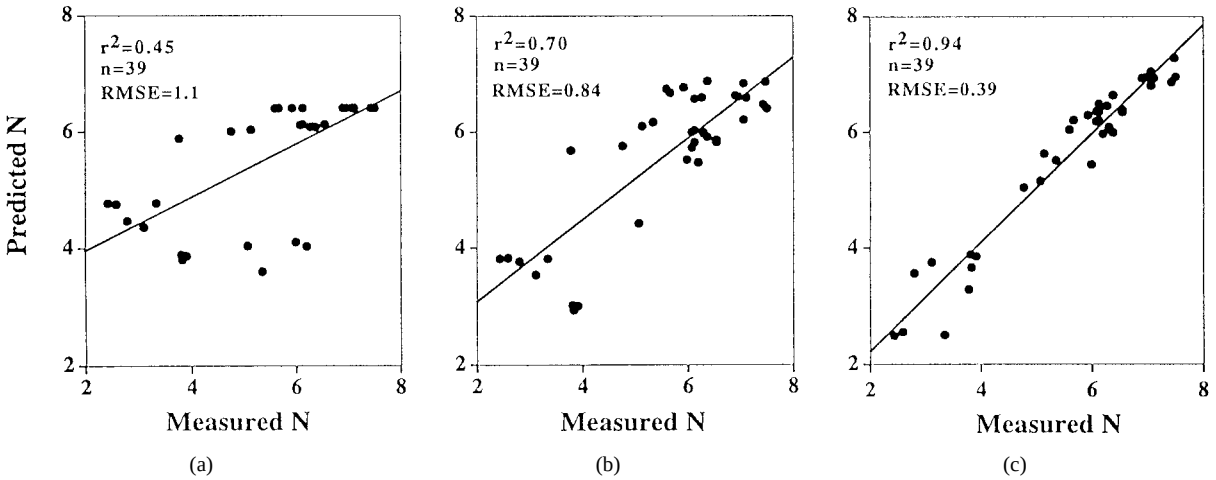

Fig. 1. Relationship between measured N concentrations and N predicted in the region off Sanriku using equations (a) $NO_3^- = -3.33 + 2.16(T) - 0.12(T)^2$ (b) $NO_3^- = -0.98 + 2.55(T) - 0.17(T)^2 - 1.57(\text{Chl } a) + 0.15(\text{Chl } a)^2$, and (c) $NO_3^- = -2101 + 948.89(T) - 17.08(T)^2 - 1.05(\text{Chl } a) + 0.11(\text{Chl } a)^2 + 2664(\log T) - 8335(\log T)^2$.

be appropriate as the coefficient of determination (r^2) for the relationship between measured and predicted N concentrations was only about 0.45. The addition of chl a led to a statistically significant increase in the value of r^2 to 0.70 [Fig. 1(b)], indicating that phytoplankton can contribute in a large measure to variations in N. A further increase in the value of r^2 to 0.94 and a substantial decrease in the root mean square error (rmse) in predicted N to about 0.39 was observed on addition of $\log_{10}$ T values [Fig. 1(c)] to the predictive equation. On account of the differences in the types of source water that were seen in the Sanriku region and the large range in the values of T that were encountered during the field campaign, it appears that the addition of $\log_{10}$ T helped improve N prediction by reducing the variability in T values. These findings based on the Sanriku Field Campaign data set thus clearly underscored the need for an additional variable such as chl a that would help account for variations in N resulting from biological uptake by phytoplankton.

2) Pacific Ocean: We tested the utility of this approach over basin scales by undertaking a similar exercise for the larger data set from the Pacific Ocean. The empirical algorithm (1) for N which resulted from this analysis

$$NO_3^- = 25.22 - 1.96(T) + 0.04(T)^2 - 1.21(\text{Chl } a) - 0.05(\text{Chl } a)^2 \quad (1)$$

could account for 83% of the variation in N with an rmse of 2.4 μM irrespective of the season and region the data were collected from.

Despite the statistically significant r^2 value that resulted from the fit, model estimates for N concentrations in the equatorial waters were lower than the observed values [Fig. 2(a)]. As can be noted in Fig. 2(a), the data points constituting the equatorial region showed a marked deviation away from the least square line of fit to the entire data set. This deviation of the equatorial region data points from the rest of the Pacific ocean data can be seen best in the plot of T versus measured N (Fig. 3), where data points of high N concentrations are found in association with relatively warmer waters. This observation did not surprise us considering that unlike most of the Pacific Ocean, the initial conditions of T and N in the source water that upwells to the surface in the eastern equatorial region are quite different from that in the temperate regions [14]. Unlike the waters brought to the surface by deep winter convective mixing in the temperate region [10], upwelled waters in the eastern equatorial region, although N rich, are from much shallower waters and hence, comparatively warmer [14]. Additionally, given the low uptake rates of N by phytoplankton in this region [15], the presence of high N in the warm waters of the equatorial waters did not seem unusual.

While we had hoped that N predictions over the entire Pacific could be fulfilled by a single equation, we reckoned that disregarding this important difference between the equatorial and nonequatorial regions would result in large underestimates of N in the equatorial region.

When linear least square fits were applied to each of these regions separately, i.e., to the equatorial region (15° N to 15° S latitude) [Fig. 2(c)] and to data points outside this region (nonequatorial region) [Fig. 2(b)], the precision of N prediction for each region improved considerably. The predictive equations that resulted from treatment of the data in this fashion were as follows.

B. Non-Equatorial Region

$$NO_3^- = 25.68 - 1.97(T) + 0.04(T)^2 - 1.63(\text{Chl } a) + 0.012(\text{Chl } a)^2$$
$$r^2 = 0.89, \quad \text{RMSE} = 2.24. \quad (2)$$

Note that (2) may sometimes yield negative N values for T values ranging from 19–26 (Fig. 4). However, outside the equatorial region, measured N values for this T range are generally close to undetectable values and hence, these negative values can be considered as zero.

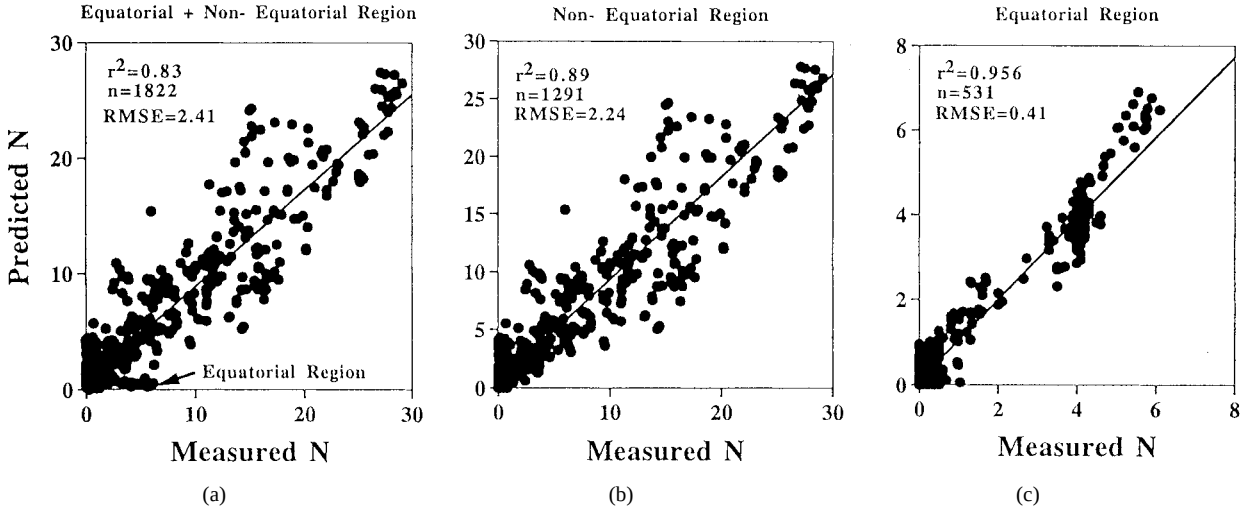

Fig. 2. Relationship between measured N and predicted N concentrations for the (a) entire Pacific Ocean, (b) nonequatorial region, and (c) equatorial region.

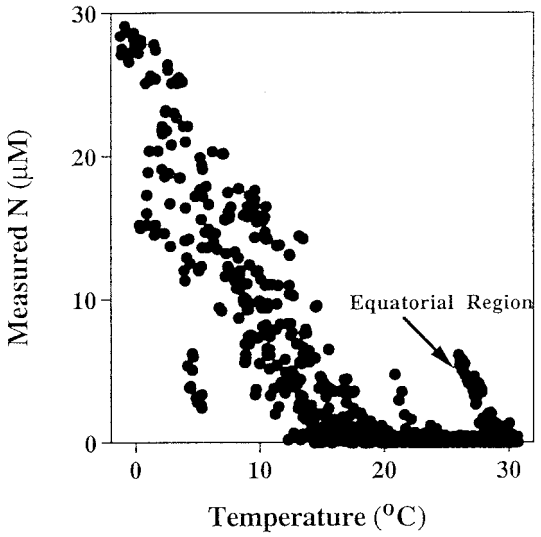

Fig. 3. Relationship between measured N and T for the entire Pacific Ocean.

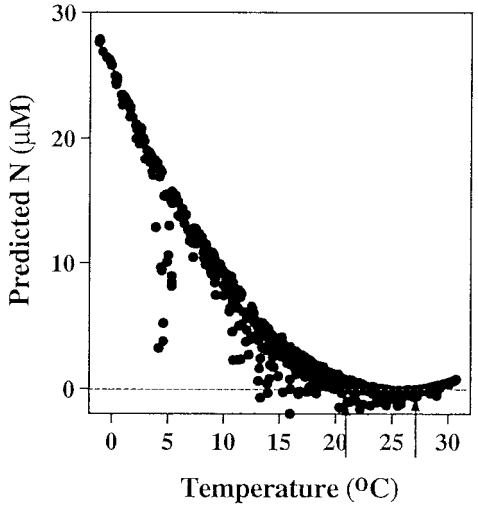

Fig. 4. Predicted N values versus T. Arrows indicate T range at which predicted N values are negative.

C. Equatorial Region

$$\mathrm{NO_3^-} = 354.47 - 23.70(\mathrm{T}) + 0.40(\mathrm{T})^2 + 3.9(\mathrm{Chl}\ a)$$
$$r^2 = 0.96, \quad \mathrm{RMSE} = 2.02. \tag{3}$$

In the equatorial region, the range of chl a values encountered fluctuated within a narrow range. Since the addition of the quadratic term for chl a yielded no improvements in the predictive capability of the algorithm, it was omitted from (3).

It can be noted that considerable differences exist in the absolute values of the parameters between (2) and (3). A difference that is particularly noteworthy is the effect of the predictor variable chl a on the derived values of N. As is evident from (2), any increase in chl a in the nonequatorial region would contribute to a decline in N concentrations. This is understandable, since outside the subtropical gyres, phytoplankton biomass increase and its accumulation in the euphotic water column occurring during the onset and progress of blooms in the nonequatorial Pacific ocean results in rapid depletion of nutrients. As a consequence, N concentrations in the euphotic zone are generally lower when chl a values are high.

In the equatorial region, in contrast, the relationship between N and chl a is opposite (N increases with chl a increase). Reasons for the existence of a positive relationship between these two variables are not well known, but we believe that this could be related to the characteristic physical and biological features that prevail in the central and western equatorial Pacific ocean. This region is known for its high rates of seawater mixing [14]. In addition, the rates of growth and nutrient uptake by phytoplankton in this region are low [15], [16]. Under these conditions, phytoplankton seldom accumulate to attain bloom proportions that could eventually contribute to a decrease in N concentrations within the euphotic water column. It has also been hypothesized that zooplankton grazing rates and iron limitation in the equatorial Pacific waters keep phytoplankton biomass so low that rates of nutrient depletion

by phytoplankton never equal or attain higher rates than the physical supply of nutrients [16]–[18].

Due to lack of data, we are not able to state whether a similar relationship of N with chl a exists off the coast of Peru in the eastern equatorial Pacific ocean. However, the reported occurrence of diatom blooms in this region [18] strongly suggests that a comparable relationship may not be applicable here.

D. Algorithm Application

To demonstrate the utility of these least square fits in obtaining N maps from satellite data over both local as well as basin scales, we have as examples applied the equations to both local area coverage (LAC) and global area coverage (GAC) SST and chl a imagery obtained concurrently by the multichannel sensor OCTS which flew on board the ADEOS satellite. These images obtained as level 3 products (ver. 3) were processed at the Earth Observation Centre (EOC), NASDA, Japan. The LAC images have a spatial resolution of 700 m, whereas for the GAC images, the spatial resolution is about 4 km. The accuracies of the derived T values are 0.68K for SST [19] and 68% for chl a [20] for values less than 2 mg m^{-3}. Above 2 mg m^{-3}, it is suspected that the derived chl a values in the ver. 3 OCTS chl a products are underestimates of the true values due to a problem with the in-water chl a algorithm [20].

1) LAC Images: The LAC images of SST and chl a utilized in this study were obtained during a single pass of the satellite in the Sanriku region off the coast of Japan on April 26, 1997. These images were selected because they had the lowest percentage of cloud cover and were closest in time to the Sanriku Field Campaign period, undertaken roughly ten days later. As the region off Sanriku is in the temperate zone, the nonequatorial equation (2) was applied to derive N concentrations.

Two features in the image of N presented (Fig. 5) are particularly noteworthy and encouraging: 1) N concentrations in the image are well within the range of those obtained during the field campaign, and 2) N concentrations associated with the different water masses that characterize the region off Sanriku are clearly discernible. The extent of N rich (>12 μM) Oyashio waters in the north, the intrusion of the N poor (<3 μM) waters of the Kurshio northward extension into the Oyashio, and the presence of moderately high N concentrations (between 3 and 12 μM) in the mixed waters at the Kursohio–Oyashio confluence and in the warm core ring can be clearly seen in the N image. The distribution of N along the section surveyed during the field campaign [11] shows a strong resemblance with the spatial trends observed in the satellite data. However, as is apparent from this study off Sanriku, even when the survey area under investigation is small, ship data alone may not be adequate in providing a clear picture of N rich and poor regions, especially when the water masses are varied and their circulation patterns are dynamic and complex. The image of N that we have presented (Fig. 5) here shows that remotely sensed data could be utilized effectively to extend the resolution of shipboard data and, therefore, provide a much clearer picture of N distribution not possible by shipboard data alone.

2) GAC Images: GAC images of N concentrations for two months,, i.e., April and June 1997 [Fig. 6(a) and (b)], are shown as examples to depict the applicability of the least square fit equations for basin scale measurements of N. Both SST and chl a images used for deriving the global maps of N were obtained from daily GAC images which were first composited over a week to minimize cloud cover and reduce gaps in the data. The weekly images were then averaged over a month to produce monthly satellite GAC, SST, and chl a images. All this processing was undertaken at the EORC, NASDA, Japan. The choice of satellite data for these months was determined largely by the availability of N data for these two months on board the Skaugran Trans-Pacific cruises [27], which provided a basis for preliminary inspection and comparison with the spatial trends in N values observed in the satellite data. An additional reason which prompted our use of the satellite data for these months was that N values for April and June approximate prebloom and midbloom concentrations, respectively, in the northern Pacific Ocean.

Maps of surface water N for the months of April and June, 1997, depict the distribution of N at the start and midway through the annual spring phytoplankton bloom that occurs in the northwestern Pacific. The map of N for April [Fig. 6(a)] allows us to immediately discern the spatial extent and magnitude of N injection into the euphotic layer that results from winter deep convective mixing prior to the onset of phytoplankton growth. An interesting feature that is obvious from the map for April is the significant west–east gradient in the distribution of N, north of the sub-Arctic front. This feature was also noted in the N data collected during the Skaugran Trans-Pacific cruises [28]. The highest concentrations of N in excess of 20 μM that can be observed in the western part of the subarctic gyre are in all probability a reflection of the intense vertical mixing and nutrient injection known to occur in the vicinity of the Aleutian and Kuril Island chains [21], [22]. The lowest concentrations of N ($\sim$12 μM) north of the subarctic front are in the region of the Alaskan gyre. South of the subarctic front, in the subtropical gyre, N concentrations show a declining trend in the subtropical gyre toward the equator to values <1 μM. In the central and eastern regions of the equatorial zone, N values are higher in the range of 3–5 μM. The distribution of N in the equatorial waters is similar to what has been documented in previous shipbased studies, which have attributed N enhancement in the eastern and central regions to the persistent upwelling occurring here [14]–[18]. This physical process results in subsurface nutrient-rich waters to be transported from the west by the equatorial undercurrent and upwelled to the surface in the eastern region. Surface currents flowing toward the west help transport a portion of these upwelled N-rich waters to the central region [14]. This westward transport of nutrient-rich water is clearly visible in the satellite map of N which shows a narrowing down of the N-rich water parcel as it is carried westwards along the equator.

A northward propagation of oligotrophy resulting from the spring bloom is obvious in the map of N for the month

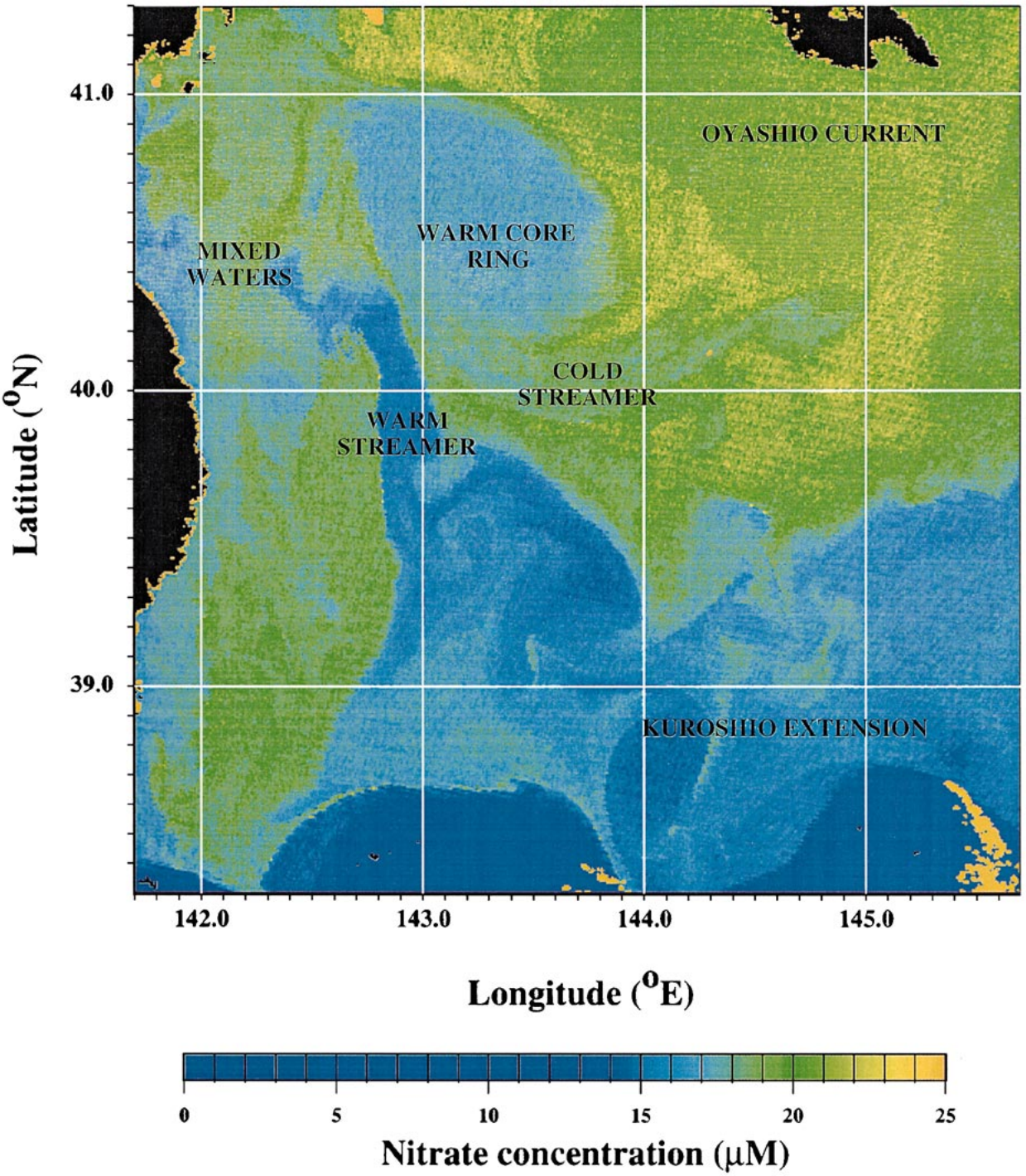

Fig. 5. LAC image of computed sea surface N in the region off Sanriku, Japan, for April 26, 1997.

of June [Fig. 6(b)]. This observation of a northward propogation of oligotrophy was also observed during cruises undertaken as part of the Northwest Pacific Carbon Cycling Study (NOPACCS) [29]. Differential amounts of insolation which contribute to differential rates of phytoplankton photosynthesis and nutrient uptake can be cited as major reasons for this north–south trend of N that can be observed in the image for June. Another noteworthy characteristic of this period is the sharper west–east gradient of N distribution compared to the month of April; the lower N concentrations resulting from the N concentrations being reduced considerably in the Alaskan gyre and the Bering Sea. Note that these concentrations of N in the Alaskan gyre and the Bering Sea are not low enough to be considered as a factor that limits the spring bloom in this region. The continued presence of high N concentrations in the subarctic Pacific Ocean at the end of the spring bloom and possible reasons for this anomaly have been reported earlier [23], [24].

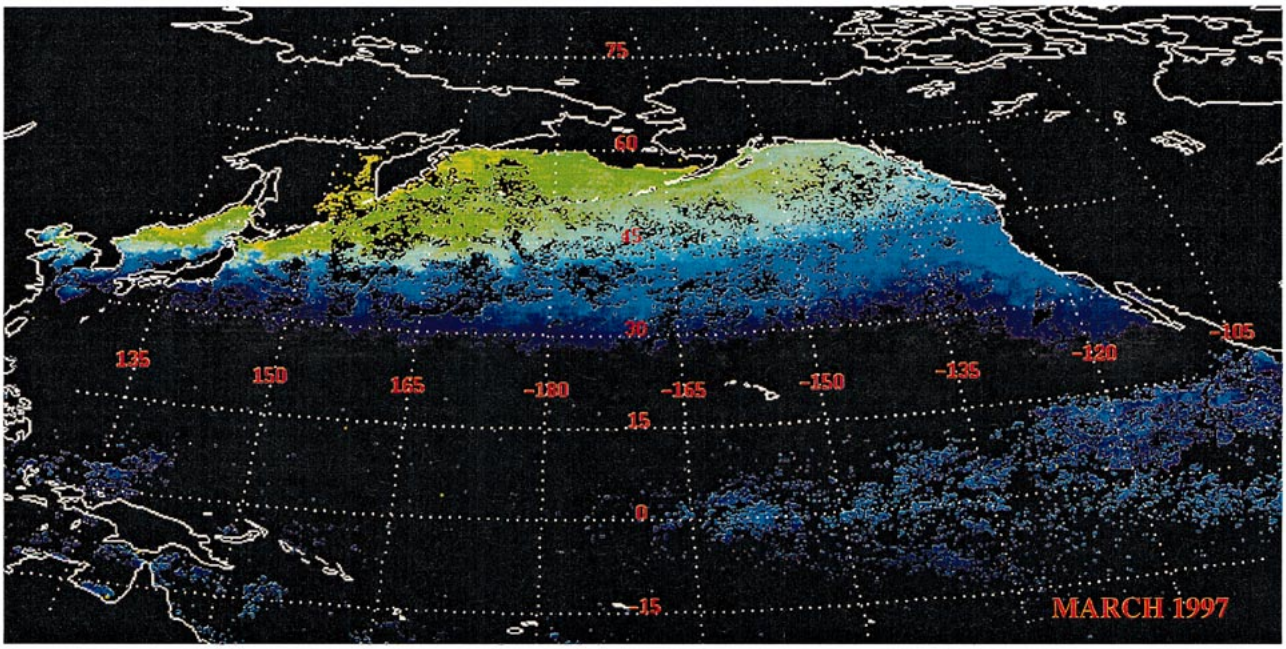

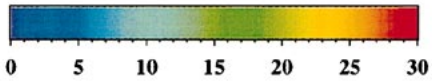

(a)

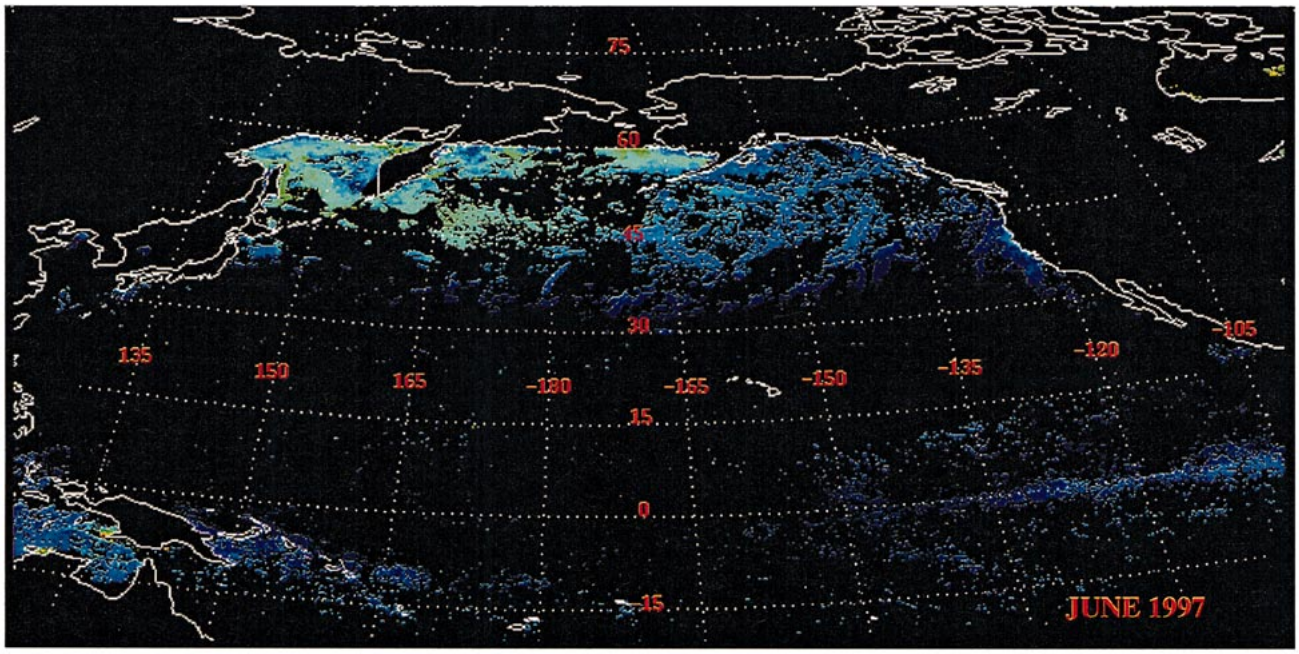

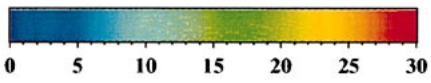

(b)

Fig. 6. GAC image of computed sea surface N for the North Pacific Ocean for the months of (a) March 1997 and (b) June 1997.

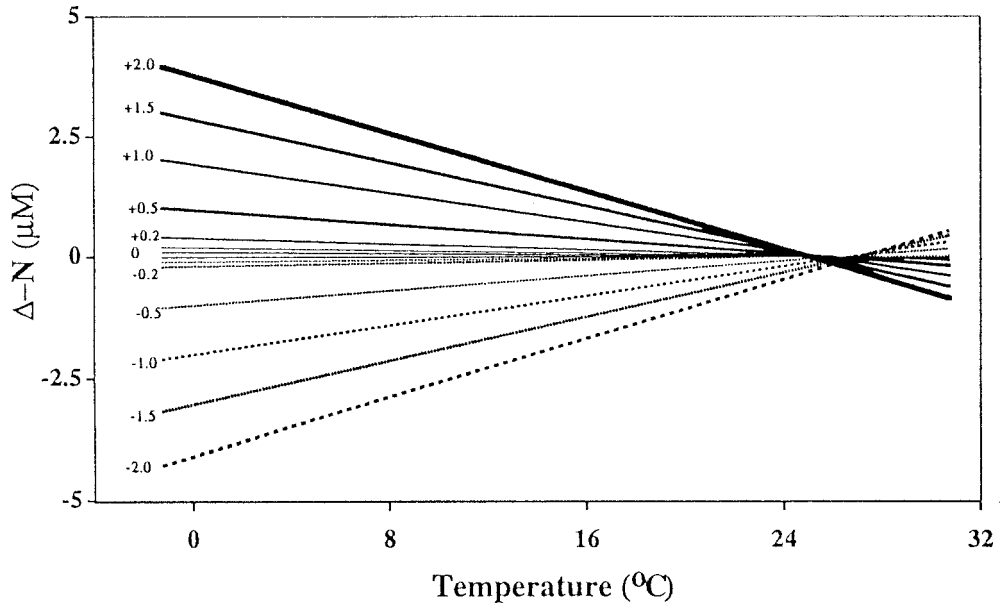

(a)

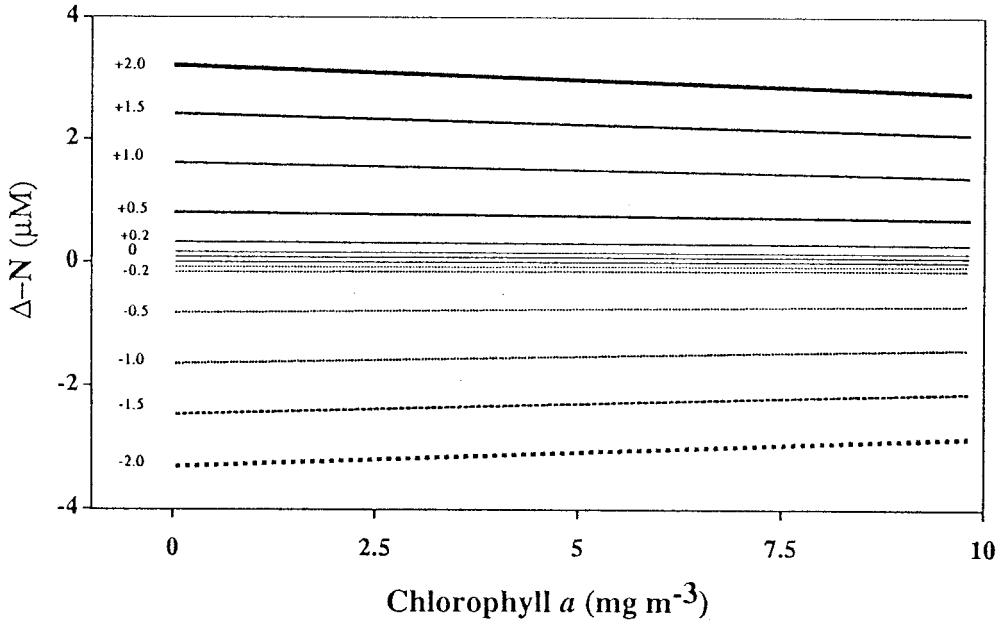

(b)

Fig. 7. (a) Effect of errors in estimates of SST on the relative error (Δ-N) in predicted N. (b) Effect of errors in chl a estimates on the predicted N. Sensitivity analysis carried out on the nonequatorial region equation (2).

3) Errors in Estimates of N from Satellites: One aspect of this study that needs to be considered is sources that could contribute to errors in N estimation from space. Errors that were associated with fitting of equations to shipboard data have been dealt with above. It does seem pertinent to mention, however, that although the shipboard data set used for developing these empirical algorithms is biased toward the central and western equatorial regions, the trends in N observed from the satellite maps are coherent with shipboard findings and are thus encouraging as a first step toward our goal of determining N from space. We hope that our future work with a larger data set of shipboard measurements covering a wider range of water types will help in refining the N predicting algorithms presented in this study.

Deviations from precision in shipboard measurements and biases in satellite estimates of SST and chl a data are additional factors that could also directly contribute to uncertainties in satellite-based N estimates. With substantial improvements in shipboard instrumentation and analytical methods made over the last several years, experimental errors that could result from shipboard data are expected to be minimal. One expects that the largest source of error in remote sensing of N could be related to errors in satellite estimates of SST and chl a themselves.

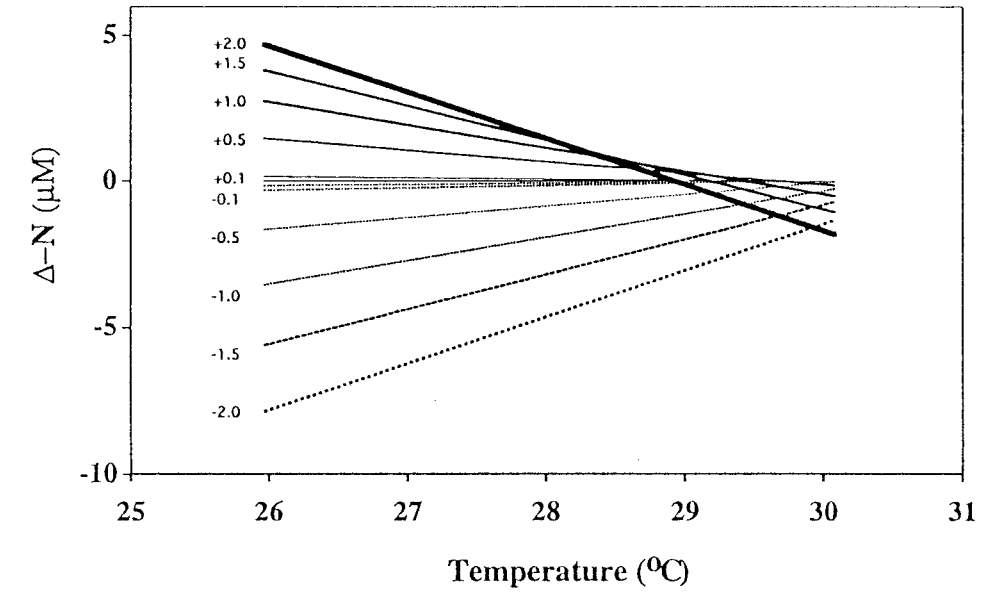

(a)

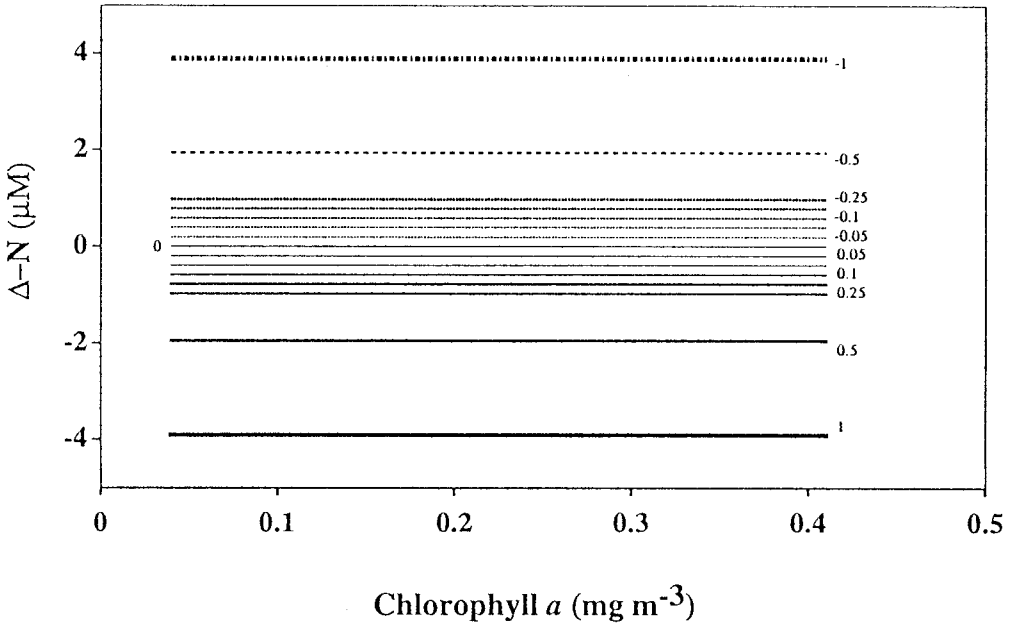

(b)

Fig. 8. Same as Fig. 6(a) and (b) but for the equatorial region equation (3).

We examined our equations for sensitivity to possible errors in satellite estimates of SST and chl a through systematic positive and negative increments in SST and chl a values, separately at first, and then in combination. The results of this exercise are presented in Figs. 7–10.

Figs. 7(a) and 8(a) show the margin of error in estimates of N (Δ-N) that could result from errors in satellite estimates of SST ranging from -2 to 2 °C for the nonequatorial and equatorial regions, respectively. In both Figs. 7(a) and 8(a), it can be noted that the largest errors ($\sim$5 μM) in N estimates would result at the lower end values of T that are typical for each region. For the nonequatorial region [Fig. 6(a)], it can be seen that the greatest errors in N due to either an overestimate or underestimate in satellite SST values can be expected at T values below 0 °C; the margin of error declining toward higher T values. For the equatorial waters, Fig. 7(a) shows that the greatest errors in N estimates can be expected at around 26 °C, close to the lowest T values in the shipboard data set used in this study, declining toward higher T values. The accuracy [19] of SST estimated by the OCTS was within 0.68 K, and therefore, it can be expected that the maximum error in remotely derived N values that could result from errors in estimates of satellite SST would be well within 1 μm for the entire range of oceanic SST's.

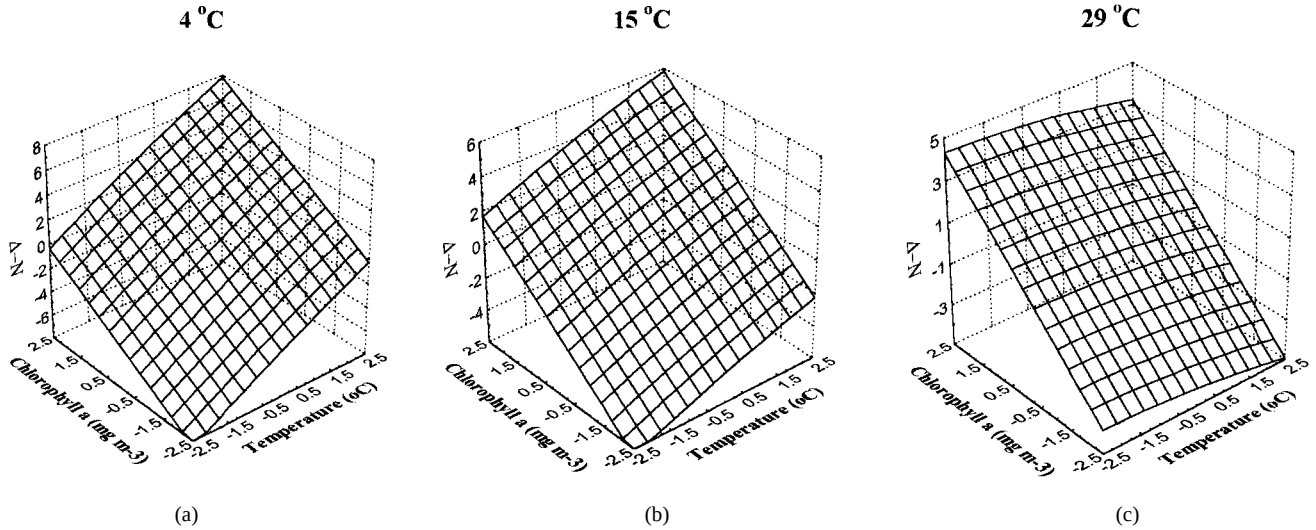

Fig. 9. (a)–(c) Combined effects of changing SST and chl a estimates on the relative error in estimated N at three different temperatures. This sensitivity analysis has been carried out on (2). (a) 4 °C, (b) 15 °C, and (c) 29 °C.

Figs. 7(b) and 8(b) depict errors in estimates of N that could result from errors in satellite estimates of chl a. For both the nonequatorial and equatorial regions, it can be seen that for values of chl a ranging from negligible to 2 mg m^{-3}, errors in N resulting from errors in satellite estimates of chl a would be much lower as compared to errors resulting from errors in SST estimates. Given that the accuracy of chl a estimates [19] by the OCTS (ver. 3) is about 68% for chl a concentrations less than 2 mg m^{-3}, in the nonequatorial region, this would result in an error in N estimates of $\sim$2 μM for chl a concentrations less than 2.5 mg m^{-3}. In contrast, for the entire range of chl a encountered in the western and central equatorial regions, this would translate into a Δ-N value of within 1 μM [Fig. 8(b)]. Also note that while an overestimate in chl a in the nonequatorial region leads to N being underestimated, in the equatorial region the effect of chl a is opposite.

Errors in satellite estimates of N that would result from a combination of errors in satellite estimates of SST and chl a at three different ambient T values of sea water have been presented in Fig. 9(a)–(c) for the nonequatorial region and Fig. 10(a)–(c) for the equatorial region. It is evident from this analysis that errors in satellite estimates of N would be far greater when both SST and chl a estimated by the satellites are in error. Based on this analysis, it follows that in the nonequatorial region, the greatest errors could result when both SST and chl a are underestimated or when both SST and chl a are overestimated by satellites [Fig. 9(a), (b)]. Note, however, that this trend is not similar when the actual SST of seawater is high $\sim$29 °C [Fig. 9(c)]. From Fig. 8(a)–(c), it is also clear that the margin of error in N estimates by satellites would be far greater at very low or high ambient SST's [Fig. 8(a), (c)] than at middle ambient SST's [Fig. 9(b)]. It is also apparent that if SST and chl a are underestimated, N would also be underestimated, but a combination of an overestimate and underestimate of these two variables would reduce the magnitude of error in the estimates at low and middle SST's. As can be seen in Fig. 10(a)–(c), the equatorial region equation is much more sensitive to errors in SST and chl a estimates than the nonequatorial equation, the greatest errors in N estimates resulting at lower end T values [Fig. 10(a), (b)]. However, it may be noted that in contrast to the nonequatorial region, a combination of an underestimate in chl a and an underestimate in SST would reduce the margin of error in N but only at ambient T values below 30 °C.

IV. Summary and Conclusions

Previous studies have demonstrated the possibility of constructing maps of sea surface water N based solely on satellite SST but, over very restricted areas [5]–[7] because of the instability of T-N relationships over larger space and time domains. It has been reported that variations in the character of T-N result when measurements from deeper waters are included in the relationship. When treated in this fashion, T-N relationships are dominated by signatures from deeper waters and any changes that result from seasonal patterns of solar radiation and phytoplankton uptake appear as noise [5]. Restricting our analysis to near surface and surface waters helped overcome this problem. The inclusion of chl a also contributed to improvement of the predictive algorithms by reducing local and regional differences in T-N relationships that could result from biology.

It may be noted, however, that satellite N estimates cannot be expected to and will not match accuracies attainable by shipboard measurements, but at best will represent "potential" N values. This is particularly true as long as satellite estimates of SST and chl a are in error. For this reason, it is to be noted that satellite data are not and should not be considered as a substitute for shipboard measurements, but rather as a tool for providing synoptic information on variability in seawater N concentrations when such data is difficult to attain by ship-based observations alone. This capability is particularly important in regions such as the subpolar regions

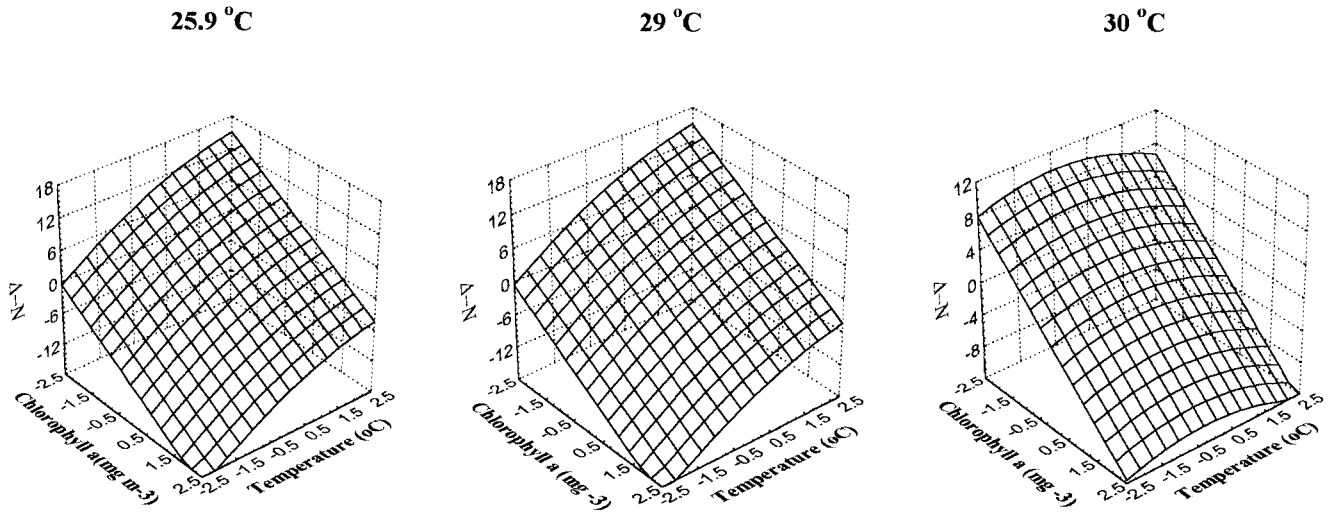

Fig. 10. (a)–(c) Combined effects of changing SST and chl a estimates on the relative error in estimated N at three different temperatures. This sensitivity analysis has been carried out (3). (a) 25.9 °C, (b) 29 °C, and (c) 30 °C.

in winter, when shipboard cruises are difficult to conduct, and the problem of undersampling is acute. In areas close to land masses where the physical boundaries of the water masses are more diverse and dynamic to be understood by shipboard measurements alone, satellite data could be particularly invaluable. One expects that as satellite-based estimates continue to improve, and shipboard data sets with greater precision become available, errors in N estimates from space will be minimized and their utility immensely enhanced.

This study is a first endeavor at demonstrating the merits of utilizing concurrent satellite imagery of SST and chl a for measuring variables which have no special electromagnetic signatures that could be used for their direct estimation from space. Due to the unexpected loss of the ADEOS, there is no satellite in space at present which can provide coregistered images of SST and chl a, as was possible by the OCTS. However, our ongoing work with SST imagery from the National Oceanic and Atmospheric Administration (NOAA), Advanced Very High Resolution Radiometer (AVHRR) and chl a from the Sea-viewing Wide Field of view Sensor (Sea-WiFS) has convinced us that a similar approach could be applied to these images to produce high-resolution maps of sea surface N. It is certain that further research will demonstrate the extendibility of our compound remote sensing method to other oceanic basins and to estimating other elements which are of importance to marine food chain, marine biogeochemical cycling studies, and climate research. When dealing with these processes on basin and global scales, any information that can be obtained from satellites has several obvious advantages over conventional methods [25], [26].

ACKNOWLEDGMENT

The authors are thankful to Dr. I. Asanuma of the Japan Marine Science and Technology Center, Kanagawa, Japan, and Dr. J. Ishizaka of the National Institute for Resources and Environment, Tsukuba, Japan, for permission to use their data and to Dr. Y. Nojiri, National Institute for Environmental Studies, Tsukuba, Japan, for helpful discussions during the course of this study. They express their gratitude to the Dr. E. DeSa, Director, National Institute of Oceanography, Goa, India, for his kind permission to J. I. Goes to collaborate in this work.

REFERENCES

[1] R. W. Eppley and B. J. Peterson, "Particulate organic matter flux and planktonic new production in the deep ocean," *Nature*, vol. 282, pp. 677–680, 1979.

[2] T. Platt, W. G. Harrison, M. R. Lewis, W. K. W. Li, S. Sathyendranath, R. E. Smith, and A. F. Vezina, "Estimating new production in the sea—A case for a consensus," *Mar. Ecol. Prog. Ser.*, vol. 52, pp. 77–88, 1989.

[3] S. Sathyendranath, T. Platt, W. P. W. Horner, W. G. Harrison, O. Ulloa, and R. Outerbridge, "Estimation of new production in the ocean by compound remote sensing," *Nature*, vol. 353, pp. 129–133, 1991.

[4] F. P. Chavez and S. K. Service, "Temperature-nitrate relationships in the central and eastern tropical Pacific," *J. Geophys. Res.*, vol. 101, no. C9, pp. 20 553–20 563, 1996.

[5] C. Garside and J. C. Garside, "Euphotic-zone nutrient algorithms for the NABE and EqPac study sites," *Deep-Sea Res.*, vol. 42, pp. 335–347, 1995.

[6] D. Kamykowski and S. J. Zentara, "Predicting plant nutrient concentrations from temperature and sigma-*t* in the upper kilometer of the world ocean," *Deep-Sea Res.*, vol. 33, pp. 89–105, 1986.

[7] E. D. Traganza, V. M. Silva, D. M. Austin, W. L. Hanson, and S. H. Bronsink, "Nutrient mapping and recurrence of coastal upwelling centers by satellite remote sensing: Its implication to primary production and the sediment record," in *Coastal Upwelling*, E. Suess and J. Thiede, Eds. New York: Plenum, 1983, pp. 61–83.

[8] R. C. Dugdale, A. Morel, A. Bricaud, and F. P. Wilkerson, "Modeling new production in upwelling centres: A case study of modeling new production from remotely sensed temperature and color," *J. Geophys. Res.*, vol. 94, no. C12, pp. 18 199–18 132, 1989.

[9] P. Morin, M. V. M. Wafar, and P. Le Corre, "Estimation of nitrate flux in a tidal front from satellite-derived temperature data," *J. Geophys. Res.*, vol. 98, no. C3, pp. 4689–4695, 1993.

[10] D. Kamykowski, "A preliminary biophysical model of the relationship between temperature and plant nutrients in the upper ocean," *Deep-Sea Res.*, vol. 34, pp. 1067–1079, 1987.

[11] T. Saino and H. R. Gomes, "ADEOS field campaign off Sanriku/North Pacific, May 7–14, 1997, *R./V. Tansei Maru*," Tech. Rep., Institute for Hydrospheric-Atmospheric Sciences, Nagoya University, Japan, 1997.

[12] D. Inagake and S. Saitoh, "Description of the oceanographic conditions and its relation to the spring bloom detected by OCTS images around the Kuroshio/Oyashio mixed water region," *J. Ocean.*, vol. 54, pp. 479–494, 1998.
[13] H. R. Gordon and A. Y. Morel, *Remote Assessment of Ocean Color for Interpretation of Satellite Visible Imagery*. New York: Springer-Verlag, p. 114, 1983.
[14] F. Chai, S. T. Lindley, and R. T. Barber, "Origin and maintenance of a high nitrate condition in the equatorial Pacific," *Deep-Sea Res.*, vol. 43, pp. 1031–1064, 1996.
[15] J. H. Martin and the IronEx Team, "Testing the iron hypothesis in ecosystems of the equatorial Pacific Ocean," *Nature*, vol. 371, pp. 123–129, 1994.
[16] J. J. Cullen, M. R. Lewis, C. O. Davis, and R. T. Barber, "Photosynthetic characteristics and estimated growth rates indicate grazing is the proximate control of primary production on the equatorial Pacific," *J. Geophys. Res.*, vol. 97, pp. 639–654, 1992.
[17] M. R. Landry, J. Constantinou, and J. Kirshtein, "Microzooplankton grazing in the central equatorial Pacific during Feb. and Aug. 1992," *Deep-Sea Res.*, vol. 33, pp. 657–672, 1995.
[18] R. T. Barber and F. P. Chavez, "Regulation of primary productivity rate in the equatorial Pacific," *Limnol. Oceanogr.*, vol. 36, pp. 1803–1815, 1991.
[19] F. Sakaida, E. Moriyama, H. Murakami, H. Oaku, Y. Mitomi, A. Mukaida, and H. Kawamura, "The sea surface temperature product algorithm of the Ocean color and temperature scanner (OCTS)/ADEOS and its accuracy," *J. Ocean.*, vol. 54, pp. 437–442, 1998.
[20] M. Shimada, H. Oaku, Y. Mitomi, H. Murakami, A. Mukaida, J. Ishizaka, H. Kawamura, T. Tanaka, M. Kishino, and H. Fukushima, "Calibration and validation of the ocean color version 3 product from ADEOS OCTS," *J. Ocean.*, vol. 54, pp. 401–416, 1998.
[21] T. Kono, "Modification of the Oyashio water in the Hokkaido and Tohoku areas," *Deep Sea Res.*, vol. 44, pp. 669–688, 1997.
[22] K. Kitani, "An oceanographic study of the Okhotsk Sea—Particularly in regard to cold waters," *Bull. Far Seas Fish. Res. Lab.*, vol. 9, pp. 45–77, 1973.
[23] C. B. Miller, B. W. Frost, P. A. Wheeler, M. R. Landry, N. Welschmeyer, and T. M. Powell, "Ecological dynamics in the subarctic Pacific, a possible iron-limited ecosystem," *Limnol. Oceanogr.*, vol. 36, pp. 1600–1615, 1991.
[24] P. A. Wheeler and S. A. Kokkinakis, "Ammonium recycling limits nitrate use in the oceanic subarctic Pacific," *Limnol. Oceanogr.*, vol. 35, pp. 1267–1278, 1990.
[25] T. Platt, C. Caverhill, and S. Sathyendranath, "Basin-scale estimates of oceanic primary production by remote sensing: The North Atlantic," *J. Geophys. Res.*, vol. 96, no. C8, pp. 15 147–15 159, 1991.
[26] A. Morel and J. F. Berthon, "Surface pigment, algal biomass profiles, and potential production of the euphotic layer: Relationships reinvestigated in view of remote-sensing applications," *Limnol. Oceanogr.*, vol. 34, pp. 1545–1562, 1989.
[27] Y. Nojiri and C. S. Wong, unpublished data.
[28] ——, personal communications.
[29] J. Ishizaka, unpublished data.

Joaquim I. Goes received the M.S. degree in microbiology from the University of Bombay, India, and the Dr.Sci. degree in marine biogeochemistry from Nagoya University, Japan. As part of his Doctoral dissertation, he studied the effects of enhanced UV-B radiation on the patterns of carbon assimilation in marine phytoplankton.

He is currently a Japan Society for Promotion of Science postdoctoral fellow at the Institute for Hydrospheric and Atmospheric Sciences (IHAS), Nagoya University, Nagoya, Japan, on secondment from the National Institute of Oceanography, India , where he works as a Research Scientist in the Biological Oceanography Division. His main research interests include ocean color remote sensing, bio-optics, phytoplankton physiological-ecology, marine biogeochemistry, and food web studies.

Toshiro Saino received the D.S. degree from Graduate School of Science, University of Tokyo, Tokyo, Japan, in 1978.

He is presently a Professor at the Institute for Hydrospheric and Atmospheric Sciences, Nagoya University, Nagoya, Japan, and also a member of Invited Eminent Scientists of EORC/NASDA. He is serving as the chairman of the Ocean Biology Science Team of ADEOS Project. He represents Japan on the Science Steering Committee of the Joint Global Ocean Flux Study and is co-chairman of the North Pacific Task Team. His research interests include carbon and nitrogen isotope studies and use of sediment traps in conjunction with ocean color remote sensing for studying the regulating mechanisms of biological processes in global material cycling in the ocean.

Hiromi Oaku received the B.S. and M.S. degrees in physics in 1991 and 1993, respectively, from the Physics Department, University of Tokyo, Tokyo, Japan.

Since 1993, she has been working at NASDA's Earth Observation Center and Earth Observation Research Center, Tokyo, where she was responsible for calibrating and validating spaceborne data from the JERS-1 SAR, ADEOS OCTS, and AVNIR.

Ding Long Jiang was born in Heilongjiang Province, China. He received the B.S. degree in physics from Dalian University of Technology, China, in 1992.

Thereafter, he worked at the Department of Hydraulics, China Institute of Water Conservancy and Hydroelectric Power Research, Beijing, until September 1996. He is presently on a Ministry of Education, Science, Sports and Culture (Monbusho), Japan scholarship at the Institute for Hydrospheric and Atmospheric Sciences, Nagoya University, Nagoya, Japan, where he is studying for the M.S. degree under UNESCO's International Hydrosphere Programme.